

SCIENTIFIC REPORTS



OPEN

Comparison of AOD from CALIPSO, MODIS, and Sun Photometer under Different Conditions over Central China

Boming Liu¹, Yingying Ma^{1,2}, Wei Gong^{1,2}, Ming Zhang¹, Wei Wang¹ & Yifan Shi¹

Cloud-Aerosol Lidar and Infrared Pathfinder Satellite Observation (CALIPSO) provides three-dimensional information on aerosol optical properties across the globe. However, the performance of CALIPSO aerosol optical depth (AOD) products under different air quality conditions remains unclear. In this research, three years of CALIPSO level 2 AOD data (November 2013 to December 2017) were employed to compare with the Moderate Resolution Imaging Spectroradiometer (MODIS) level 2 columnar AOD products and ground-based sun photometer measurements for the same time period. To investigate the effect of air quality on AODs retrieved from CALIPSO, the AODs obtained from CALIPSO, MODIS, and sun photometer were inter-compared under different air quality conditions over Wuhan and Dengfeng. The average absolute bias of AOD between CALIPSO and sun photometer was 0.22 ± 0.21 , 0.11 ± 0.07 , and 0.14 ± 0.13 under clean, moderate, and polluted weather, respectively. The result indicates that the CALIPSO AOD were more reliable under moderate and polluted days. Moreover, the deviation of AOD between CALIPSO and sun photometer was largest (0.23 ± 0.21) in the autumn season, and lowest (0.13 ± 0.12) in the winter season. The results show that CALIPSO AOD products were more applicable to regions and seasons with high aerosol concentrations.

Aerosols have a significant influence on global climate change by directly altering solar radiation or indirectly modifying the cloud properties^{1–3}. However, estimation of aerosols' radiative force is uncertain due to a lack of knowledge of height-revolved optical properties^{4–7} and the nonhomogeneous spatial distribution of aerosol particles⁸. A variety of satellite sensors, such as Moderate Resolution Imaging Spectroradiometer (MODIS), Multi-angle Imaging Spectroradiometer (MISR), and Visible Infrared Imaging Radiometer Suite (VIIRS), have been used for long-term continuous detection of aerosol optical depth (AOD)^{9–11}. However, due to the limitations of passive satellite measurement, they can only provide the total column value and not the vertical distribution information for aerosols, which is important for assessment of aerosol radiative effects¹². The Cloud-Aerosol Lidar and Infrared Pathfinder Satellite Observation (CALIPSO) was developed to provide atmospheric vertical profile detecting capabilities to fill the current observation gap¹³.

The CALIPSO instrument can detect the atmospheric vertical profile at one depolarization and two scattering channels¹⁴. Information on the vertical distribution of clouds and aerosols is necessary to improve the estimation accuracy of direct and indirect radiative forcing by aerosols, and to assess the feedback of clouds within the climate system¹⁵. Currently there are many studies comparing CALIPSO vertically integrated extinction with AODs from other satellite sensors (MODIS and MISR), as well as the ground-based Aerosol Robotic Network (AERONET)^{16,17}. Kittaka *et al.* assessed the consistency of AODs obtained from the CALIPSO aerosol layer product version 2 and the MODIS-Aqua collection 5 from June 2006 to August 2008. They indicated that the two sensors have good correlation over ocean regions with low cloudiness¹⁸. Schuster *et al.* compared CALIPSO column AODs with ground-based AERONET sites from June 2006 to May 2009, and found that the CALIPSO dust retrievals had a larger assumed LiDAR ratio (more than 40 sr)¹⁹. Yu *et al.* compared AODs from CALIPSO, Goddard Chemistry Aerosol Radiation and Transport (GOCART) model simulations, and MODIS observations from June 2006 to November 2007, and suggested that MODIS AODs were generally larger than

¹State Key Laboratory of Information Engineering in Surveying, Mapping and Remote Sensing (LIESMARS), Wuhan University, Wuhan, China. ²Collaborative Innovation Center for Geospatial Technology, Wuhan, 430079, China. Correspondence and requests for materials should be addressed to Y.M. (email: yym863@whu.edu.cn)

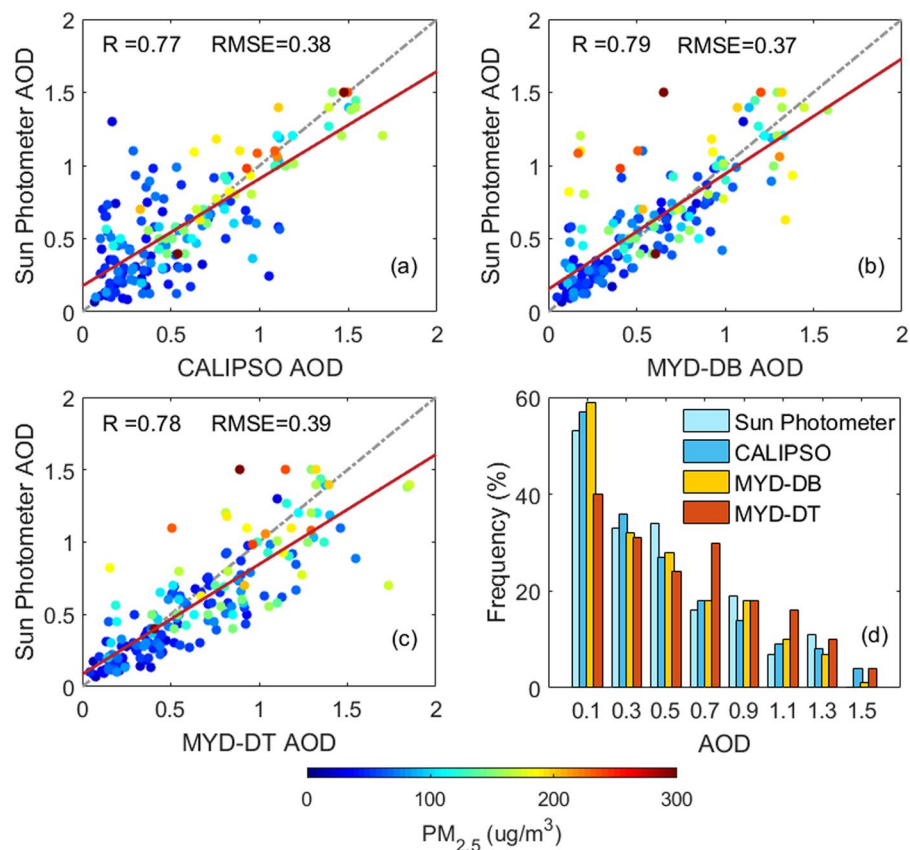


Figure 1. Scatter plots of the AODs derived from CALIPSO, MODIS, and sun photometer with change of $PM_{2.5}$ from November 2013 to December 2017. (a) CALIPSO vs. sun photometer; (b) MODIS-DB vs. sun photometer; (c) MODIS-DT vs. sun photometer; (d) frequency distribution of AODs. Color bars represent the mass concentration of $PM_{2.5}$.

CALIPSO observations over most regions²⁰. Liu *et al.* evaluated the performance of CALIPSO AOD products on the high-value regions and low-value regions, and studied the seasonal variation of AOD products over China²¹. Such comparisons provide valuable insights into the application of CALIPSO products.

With the increase in anthropogenic emissions and the advancement of urbanization, dust and haze pollution occur frequently over central China²². More and more studies have used the AOD products on the environmental research^{3,5,11}. Wang and Ma *et al.* employed the satellite AOD data to derive the $PM_{2.5}$ ^{23,24}. These studies all require a good accuracy of AOD data. But some studies have indicated that the degree of air pollution would affect satellite AOD inversion²⁵. Li *et al.* compared MODIS and AERONET AODs over China, and indicated that AODs retrieved from MODIS have larger errors in extreme aerosol conditions²⁶. Chen *et al.* evaluated the performance of the MODIS AOD product under haze-fog pollution conditions over Beijing, and pointed out that the accuracy and spatial coverage of the MODIS 3 km Dark Target AOD is poor on heavily polluted days²⁷. Therefore, it is important to assess the bias of AOD products under the different pollution level. However, there are still few studies evaluating CALIPSO AODs under different air quality conditions. The effect of air quality on CALIPSO AOD inversion needs further research, which is important for the application of CALIPSO AODs in regional environmental research.

In this work, CALIPSO AOD product was assessed by validating against the 550-nm column AOD obtained from the MODIS products and ground-based sun photometer measurements obtained at two ground sites over central China. The performance of CALIPSO AOD product was evaluated on the different $PM_{2.5}$ concentrations. When taking into consideration the effect of air quality on CALIPSO AOD inversion, we find that concentrations of fine particulate matter ($PM_{2.5}$) play an important role in the consistency of comparisons. Moreover, differences in AOD between CALIPSO and sun photometer measurements have obvious seasonal characteristics.

Results

Comparison of AODs from CALIPSO, MODIS, and Sun Photometer. Figure 1 shows scatter plots of the AODs derived from CALIPSO, MODIS, and sun photometer with change of $PM_{2.5}$. Color bars represent the mass concentration of $PM_{2.5}$. Figure 1a shows a comparison of AODs obtained from CALIPSO and sun photometer. They exhibit good correlation with each other; $R = 0.77$ and $RMSE = 0.38$. Figure 1b shows a comparison of AODs retrieved from MYD_DB and sun photometer, with $R = 0.79$ and $RMSE = 0.37$. Figure 1c shows a comparison of the AODs derived from MYD_DT and sun photometer, with $R = 0.78$ and $RMSE = 0.39$. This indicates that the AODs obtained from CALIPSO and MODIS have good correlation with the ground-based

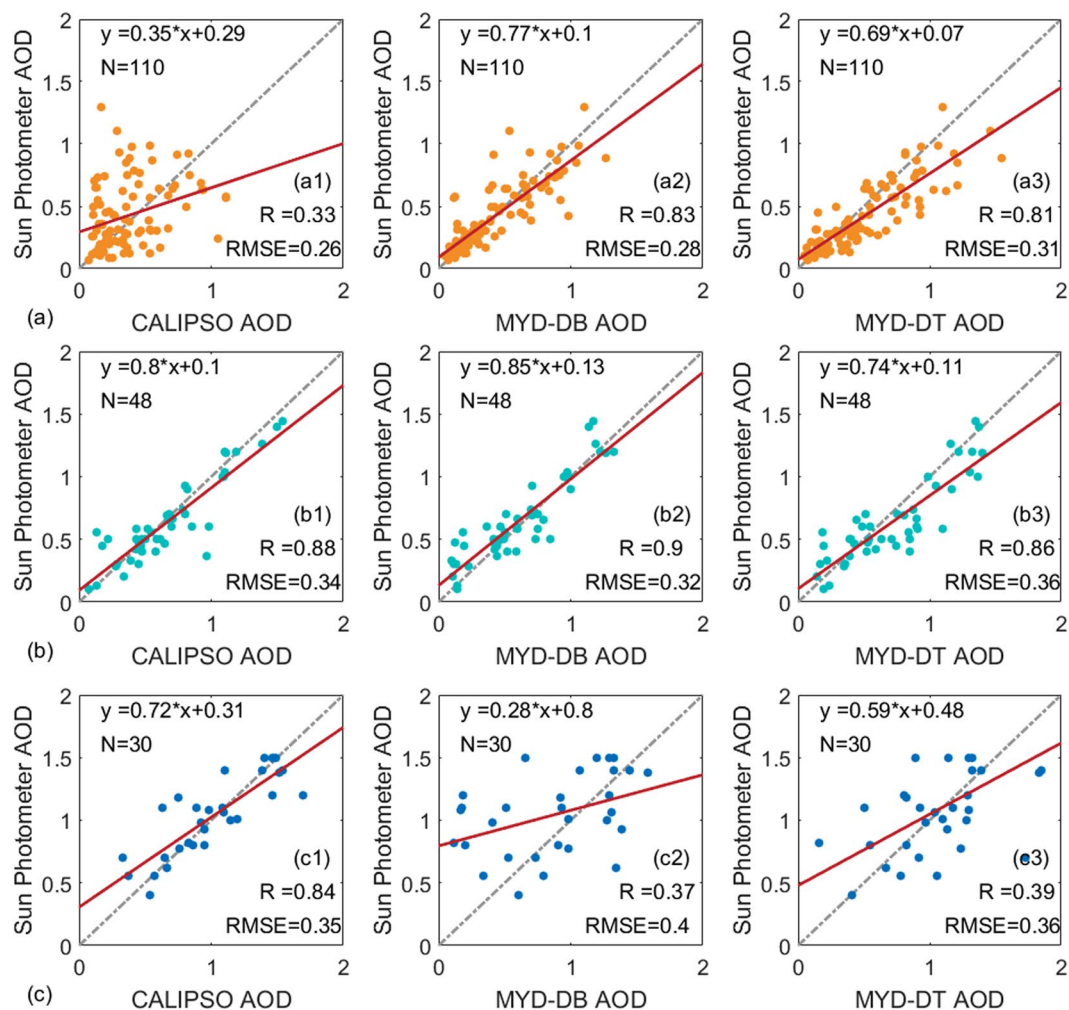


Figure 2. Scatter plots of AODs derived from CALIPSO, MODIS, and sun photometer under different air quality conditions. (a) Orange, (b) green, and (c) blue points represent sample points under clean weather, moderate air pollution, and heavy air pollution, respectively. Red and grey lines represent the linear regression curve and 1:1 reference curve, respectively.

observations. Other evaluation studies have shown similar results^{18,19}. Moreover, the color bar suggested that AODs are more similar when the mass concentration of PM_{2.5} is low. Figure 1d shows the frequency distribution of AODs retrieved from CALIPSO, MODIS, and sun photometer. The results show that their frequency distributions are similar.

Comparison of AODs under Different Air Quality Conditions. To investigate the effect of air quality on AODs retrieved from CALIPSO, the AODs obtained from CALIPSO, MODIS, and sun photometer were compared under different air quality conditions. The experimental data were divided into three subsets, based on the latest air quality standards of China (GB 3095-2012)²⁸. A 24 h average PM_{2.5} > 150.0 μg m⁻³ indicates heavy air pollution, 24 h average PM_{2.5} > 75.0 and < 150 μg m⁻³ indicates moderate air pollution, and 24 h average PM_{2.5} < 75 μg m⁻³ indicates clean air quality. According to the air quality standards of China, the experimental data were classified as 110 days of clean weather, 48 days of moderate air pollution, and 30 days of heavy air pollution.

Figure 2 shows comparisons of AODs derived from CALIPSO, MODIS, and sun photometer under different air quality conditions. Figure 2a shows a comparison of AODs derived from CALIPSO, MODIS, and sun photometer under clean weather. The correlation coefficients between CALIPSO and sun photometer, MYD_DB and sun photometer, and MYD_DT and sun photometer were R = 0.33, R = 0.83, and R = 0.81, respectively. Compared with the ground-based sun photometer, AODs retrieved from CALIPSO showed lower correlation than MODIS under clean weather. During moderate air pollution (Fig. 2b), the correlation coefficients between CALIPSO and sun photometer (R = 0.88) show obvious improvement. The correlation coefficient between MYD_DB (DT) and sun photometer reached R = 0.9 (0.86). This suggests that AODs derived from CALIPSO, MODIS, and sun photometer have good consistency under moderate air pollution. However, Fig. 2c shows that the correlation between CALIPSO and sun photometer AOD (R = 0.84) was better than that between MYD_DB/DT and sun photometer (R = 0.37/0.39) under heavy air pollution. This indicates that CALIPSO AODs exhibit poor correlation with sun photometer under clean weather. Meanwhile, the AODs retrieved from MODIS showed poor performance under

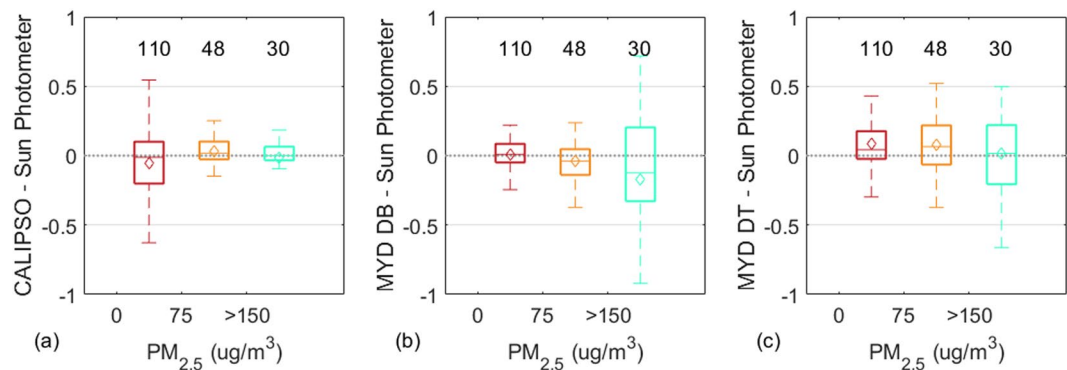


Figure 3. Box plots of AOD differences between (a) CALIPSO and sun photometer; (b) MODIS-DB and sun photometer; and (c) MODIS-DT and sun photometer with PM_{2.5} concentration change over Central China. The numbers represent the sample size of each box. The middle line and square show the median and mean value of the AOD differences, respectively.

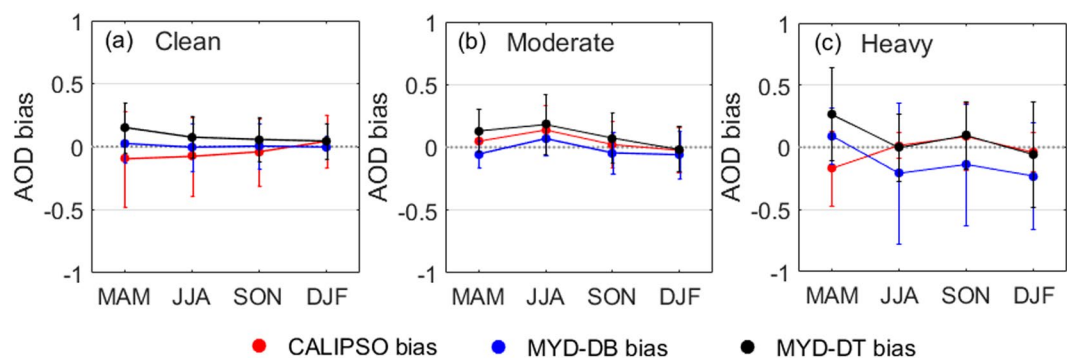


Figure 4. The seasonal deviation of AOD products under the different air quality conditions (a) The clean air quality ($PM_{2.5} < 75 \mu g m^{-3}$); (b) the moderate air pollution ($75 < PM_{2.5} < 150 \mu g m^{-3}$); and (c) the heavy air pollution ($PM_{2.5} > 150.0 \mu g m^{-3}$). The red, blue, and black lines show the CALIPSO bias, MYD_DB bias, and MYD_DT bias, respectively.

dust events or heavy urban/industrial haze. This result was similar to previously validated research, where the MODIS product exhibited poor performance under extreme aerosol conditions over East Asia^{17,20,26}.

Figure 3 shows box plots of AOD differences between CALIPSO and sun photometer, MYD_DB and sun photometer, and MYD_DT and sun photometer with PM_{2.5} concentration change over central China. Figure 3a shows that the AOD difference between CALIPSO and sun photometer was small when the PM_{2.5} concentrations was high. The AOD difference between CALIPSO and sun photometer was largest (RMSE = 0.31) in the range of 0 to 75 $\mu g m^{-3}$ PM_{2.5} concentrations. Figure 3b shows the AOD difference between MYD_DB and sun photometer with a PM_{2.5} concentration change. This indicates that the AOD difference between MODIS and sun photometer was increased with increased PM_{2.5} concentrations. The larger AOD difference (RMSE = 0.45) between MYD_DB and sun photometer was in the range of PM_{2.5} > 150 $\mu g m^{-3}$. Figure 3c shows the AOD difference between MYD_DT and sun photometer with the PM_{2.5} concentration change. It shows that the smallest AOD difference (RMSE = 0.3) between MYD_DT and sun photometer was in the range of PM_{2.5} < 75 $\mu g m^{-3}$. These results show that air quality can affect satellite AOD retrieval due to the limitations of the AOD inversion method^{11,27}. The reasons are described in the Discussion section.

Seasonal deviation of AODs under Different Air Quality Conditions. Figure 4 shows the seasonal deviation of CALIPSO, MYD_DB, and sun photometer AOD products under the different air quality conditions. Figure 4a shows that the seasonal deviation of AOD products under clean air quality. The results indicated that the seasonal variation of AOD deviations are the same under clean air quality, the deviation of AOD was smallest in winter season and largest in spring season. Figure 4b shows that the seasonal deviation of AOD products under moderate air pollution. The seasonal variation of AOD deviations is also consistent. Figure 4c shows that the seasonal deviation of AOD products under heavy air pollution. The seasonal variation of MYD_DB AOD deviations are similar with MYD_DT AOD deviations, but different with CALIPSO AOD deviations. The result shows that the deviation of CALIPSO AOD was smallest under summer (0.01 ± 0.1) and winter (-0.04 ± 0.15) season. It indicated that CALIPSO AODs were more suitable for the summer and winter season under heavy air pollution.

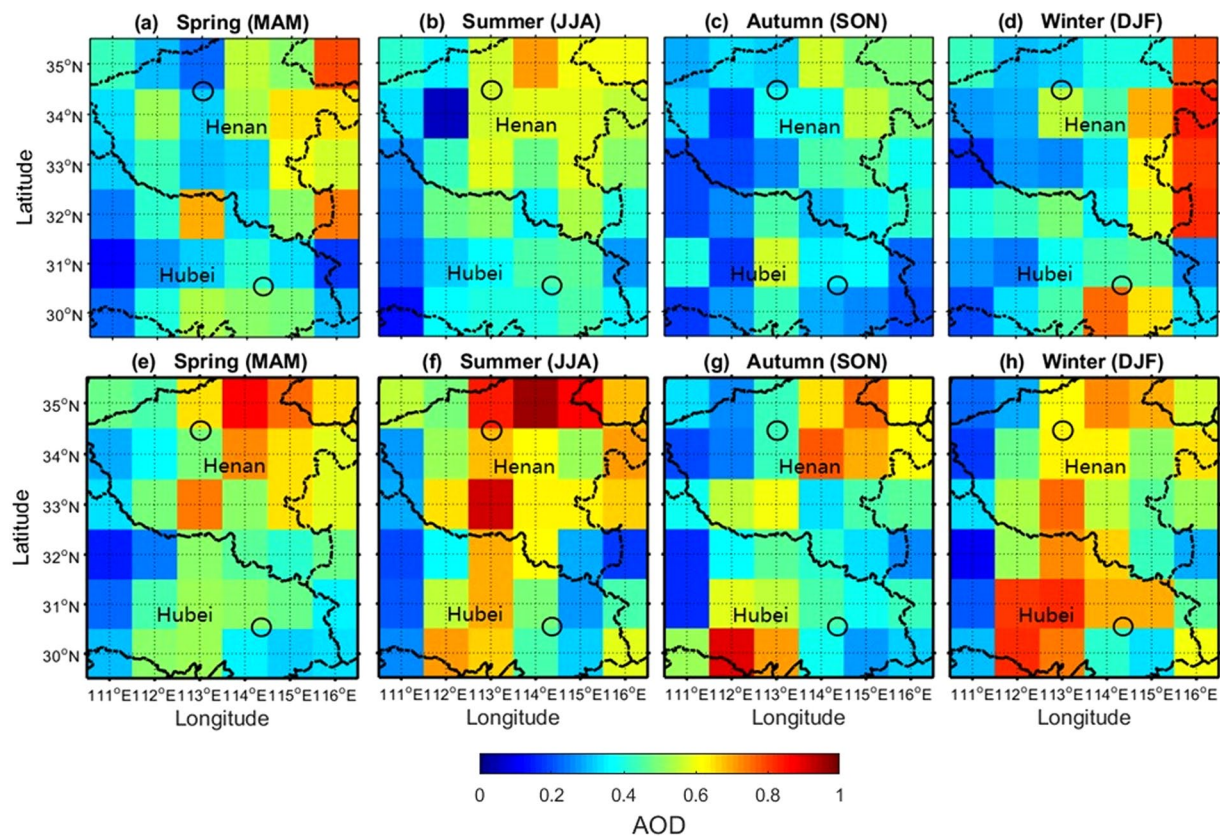


Figure 5. Seasonal mean distributions of (a–d) CALIPSO AODs and (e–h) MYD_DB AODs from November 2013 to December 2017 on $1^\circ \times 1^\circ$ equal-angle grids. Black circle represents the ground-based observation station. Spring: March, April, May; summer: June, July, August; autumn: September, October, November; winter: December, January, February.

Regional deviation of AODs. Figure 5 shows the seasonal mean distributions of CALIPSO AODs and MODIS AODs from November 2013 to December 2017 on $1^\circ \times 1^\circ$ equal-angle grids. The spatial distribution exhibited by CALIPSO was consistent with MODIS, e.g., the maximum AOD occurs over northeast Henan due to agricultural fires and anthropogenic emissions²⁹. The seasonal average of CALIPSO AOD over central China is respectively 0.438, 0.429, 0.344 and 0.396 from spring seasons to winter seasons. The mean MODIS AOD over central China is 0.529, 0.542, 0.456 and 0.482, respectively, for spring, summer, autumn and winter seasons. It is found that mean AOD over central China is high in spring and summer, and relatively low in autumn and winter. The larger AOD load during spring and summer can be attributed to the high relative humidity and anthropogenic emissions. The increasing industrial and other human activities emitted the pollutant particles. Moreover, the high relative humidity during summer may lead to hygroscopic growth of aerosol particles, resulting in larger AOD. The relatively low AOD values during spring and autumn were due to the Mongolian monsoon²². Atmospheric conditions with low pressure and high wind speed effectively promote circulation of the atmosphere, leading to a low aerosol load³⁰. However, there were some differences between CALIPSO and MODIS AODs, shown in Fig. 6.

Figure 6 shows seasonal mean differences of MODIS and CALIPSO AODs from November 2013 to December 2017 on $1^\circ \times 1^\circ$ equal-angle grids. The differences shown in Fig. 6 were defined as CALIPSO_AOD–MODIS_AOD, which describes the AOD difference between CALIPSO and MODIS retrievals. Meanwhile, the significance test ($\sigma = 0.05$) with regard to the AOD differences were conducted. The test statistics of four seasons are 6.23, 6.51, 9.43 and 3.99, respectively. All test statistics are greater than the critical value (3.98). It indicated that the AOD difference is significant. Overall, most CALIPSO AODs were systematically lower than those obtained from MODIS over Central China, especially in the Southeast Hubei and Mount Song observation station areas. Over high-pollution areas, such as East Henan, the differences between MODIS and CALIPSO AODs have obvious seasonal features. CALIPSO AODs are larger than MODIS AODs during spring and winter, and smaller in summer and autumn.

Discussion

As outlined above, the AODs retrieved from CALIPSO were assessed through a comparison with MODIS and sun photometer AODs. Overall, CALIPSO AODs are well correlated with sun photometer AODs, and can provide a solid dataset for quantitative research and air quality monitoring over central China. But AODs obtained from CALIPSO appear to have large error (>0.2) on very clean days.

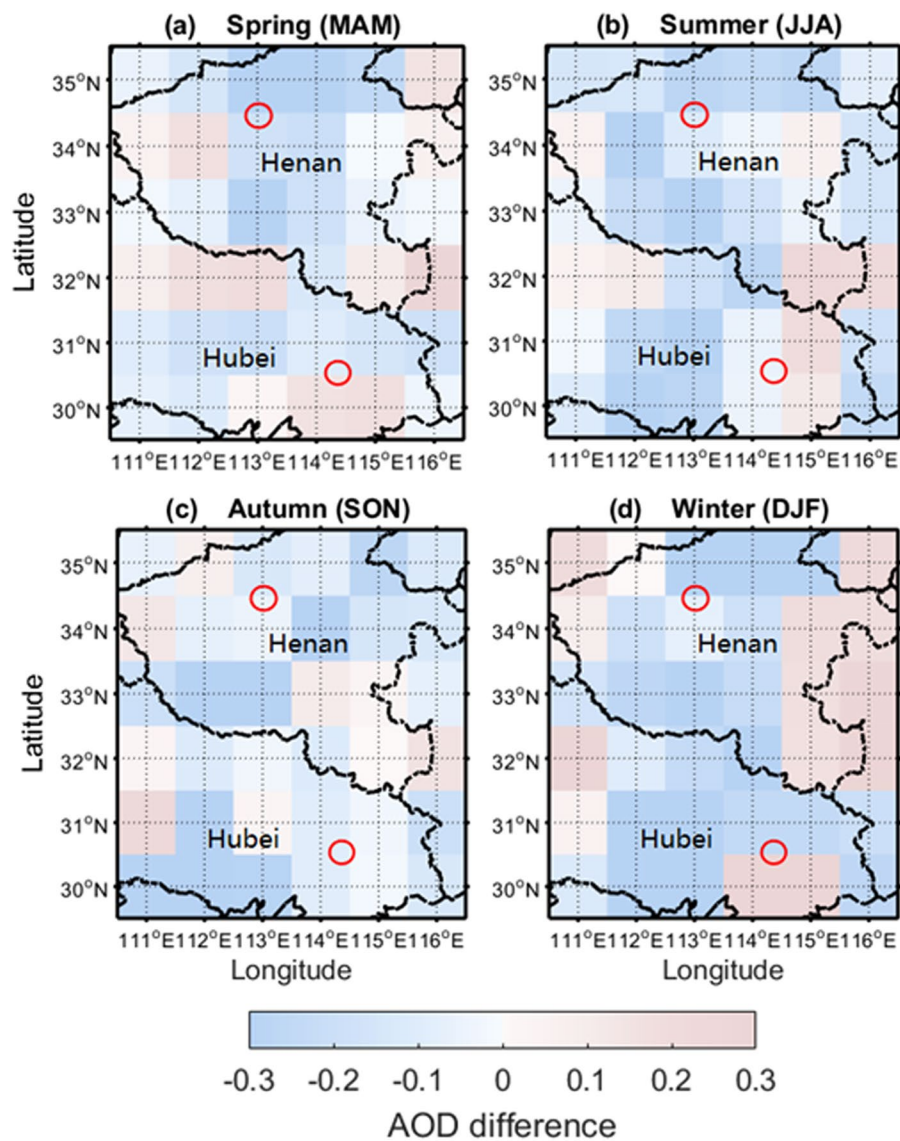


Figure 6. Seasonal mean differences of MYD_DB and CALIPSO AODs from November 2013 to December 2017 on $1^\circ \times 1^\circ$ equal-angle grids. Red circle represents the ground-based observation station. (a) Spring: March, April, May; (b) summer: June, July, August; (c) autumn: September, October, November; (d) winter: December, January, February.

Figure 7a shows the average absolute bias of AOD under different air quality conditions. Average absolute bias was relatively low on moderate pollution days. The average absolute bias of AOD between CALIPSO and sun photometer, MYD_DB and sun photometer, and MYD_DT and sun photometer was 0.11 ± 0.07 , 0.11 ± 0.1 , and 0.16 ± 0.15 , respectively. Based on ground-based observation data, the largest average absolute bias of AOD between CALIPSO and sun photometer was 0.22 ± 0.21 under clean weather. The largest average absolute bias of AOD between MYD_DB and sun photometer was 0.29 ± 0.19 under polluted conditions. The results in Figs 2 and 7a confirm that air quality does affect satellite AOD inversion. CALIPSO AODs exhibit poor correlation with sun photometer under clean weather. The AODs retrieved from MODIS showed poor performance under heavy air pollution. These differences were probably due to different AOD inversion methods^{8,17}. It should be noted that CALIPSO retrieves AOD based on the aerosol extinction vertical profile, which is classified as different types of aerosol layers by the scene classification algorithm^{31,32}. But the signal-to-noise ratio under clean weather is often too low to accurately search the weak aerosol layers on the aerosol extinction vertical profile^{8,19}. This means that highly diffuse and/or tenuous scattering aerosol layers that lie below the CALIPSO detection threshold would be ignored by CALIPSO estimates of column AOD. As a consequence, weak aerosol layers that are not detected would not be retrieved, which would result in decreased retrieved AODs under clean weather. This is also the reason that AODs obtained from CALIPSO are generally lower than those from MODIS (Fig. 6). As for the inversion of MODIS AODs, surface reflectance, single scattering albedo, and aerosol model assumptions were important input parameters in the MODIS AOD inversion algorithm^{26,27}. However, it was difficult to obtain accurate surface

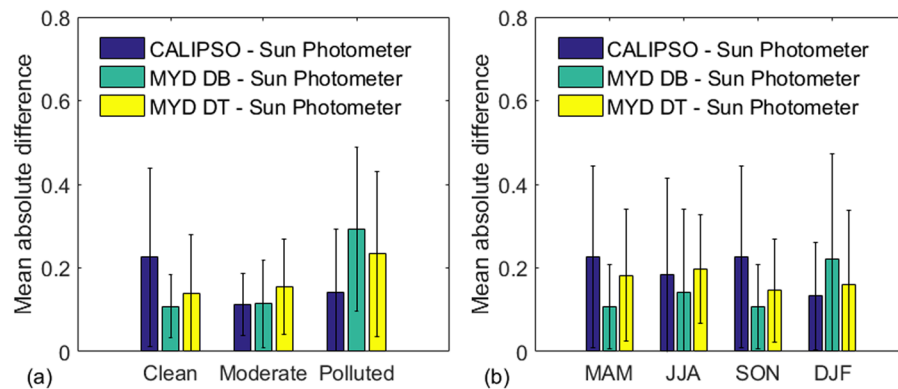


Figure 7. Average absolute bias of AODs under different conditions: (a) clean, moderate, and polluted conditions; and (b) in March, April May; June, July, and August; September, October, and November; and December, January, and February. Error bars represent standard deviations.

reflectance and single scattering albedo under heavy air pollution. Heavy industrial haze and highly concentrated secondary aerosols may have affected the input parameters in the MODIS AOD inversion algorithm²⁶. Thus, AODs retrieved from MODIS exhibited poor performance under extreme aerosol conditions. These results indicate that the CALIPSO AODs had high accuracy for moderate and polluted days over Central China.

Figure 7b shows the average absolute bias of AODs in different seasons. The largest average absolute bias of AOD between CALIPSO and sun photometer was 0.23 ± 0.21 in the autumn season, and the lowest average absolute bias was 0.13 ± 0.12 in the winter season. Due to the Mongolian monsoon during autumn^{22,30}, atmospheric conditions with low pressure and high wind speed effectively promoted circulation of the atmosphere, leading to the low aerosol load. The CALIPSO AOD over Central China was lowest (0.344) in autumn. The low AOD load may result in the larger error on AODs retrieved from CALIPSO in autumn. The relatively low average absolute bias of AOD between CALIPSO and sun photometer during the winter season can be attributed to frequent haze pollution, resulting in a high aerosol load over central China. Previous studies have indicated that the haze pollution occurred frequently under summer and winter season^{22,29}. The high aerosol load was favourable to the CALIPSO AOD inversion, but it was adverse to the MODIS AOD inversion. It was also the reason that the average absolute bias of AOD between MYD_DB and sun photometer was the largest (0.22 ± 0.25) during the winter season. The results show that CALIPSO AODs were more reliable during summer and winter than spring and autumn over central China.

Conclusions

In this study, three years of CALIPSO level 2 AOD data were employed to compare the MODIS level 2 columnar AOD products and ground-based sun photometer measurements over the same time period from November 2013 to December 2017. The results show that the AODs obtained from CALIPSO and sun photometer exhibit good correlation with each other, with $R = 0.77$ and $RMSE = 0.38$. Moreover, the air quality does affect satellite AOD inversion. The CALIPSO AOD have a larger uncertainty in clean days. The largest average absolute bias of AOD between CALIPSO and sun photometer was 0.22 ± 0.21 under clean weather. It was due to the limitation of satellite AOD inversion method. CALIPSO retrieved the AOD by the method of aerosol layer integral, which was easy to miss the thin layer, leading to the larger deviation. By contrast, the CALIPSO AOD were relatively reliable under the moderate (0.11 ± 0.07) and polluted (0.14 ± 0.13) days over central China. The enhanced aerosol layers can be effectively detected by CALIPSO, so the deviation of CALIPSO AOD was reduced with increased PM_{2.5} concentrations. Lastly, the seasonal analyses show that largest average absolute bias of AOD between CALIPSO and sun photometer was 0.23 ± 0.21 in the autumn season, and the lowest average absolute bias was 0.13 ± 0.12 in the winter season. This indicates that CALIPSO AODs were more suitable for the summer and winter season, when the haze pollution occurred frequently. On the contrary, the largest average absolute bias of AOD between MYD_DB and sun photometer was 0.29 ± 0.19 under polluted conditions. The performance of MODIS AOD was poor over heavy haze and only proposed valid data when the air is clean. In summary, When the aerosol load was relatively high over Central China, the CALIPSO AOD can provide a solid dataset for air quality monitoring. However, AODs retrieved from CALIPSO under the clean days were vulnerable to the tenuous scattering aerosol layers, and improvements and modifications are needed to achieve good accuracy.

Materials and Data

Observation Area. With rapid economic growth and population expansion, central China suffers from serious environmental and pollution problems, which have significantly increased AOD^{31,33}. To obtain enough study cases, two ground-based observation stations were used to collect the sun photometer data: Wuhan and Mountain Song. The Wuhan observation station is located at the State Key Laboratory of Information Engineering in Surveying, Mapping and Remote Sensing (LIESMARS), Wuhan University (30°32'N, 114°21'E). The sun photometer was installed on the LIESMARS roof³⁴. The Mountain Song observation station is located in Dengfeng City in Henan Province (34°31'N, 113°07'E). The sun photometer was on the roof of a building at the Songshan

observation station³⁰. The hourly mean PM_{2.5} mass concentrations were obtained from the Ministry of Environmental Protection of the People's Republic of China's observation network (<http://datacenter.mep.gov.cn/>).

AOD from Sun Photometer. The fully automated CE-318 sun photometer is a high-precision solar and sky radiation measuring instrument for use in environmental, meteorological, marine, and remote sensing applications³⁵. The instrument is mainly used to measure solar and sky radiation in visible and near-infrared wavelengths to calculate the physical and optical properties of atmospheric aerosol, as well as characteristics of atmospheric optical thickness, turbidity, water vapor, ozone, etc. Detailed instrument calibration and AOD inversion methods are described in³⁶. The uncertainty of AOD is approximately 0.01 to 0.02³⁷. Note that the sun photometer could not directly inverse the AOD at 532 nm wavelength, which matched the CALIPSO visible wavelength, so we interpolated between available sun photometer wavelengths based on the spectrum Angstrom index relationship to get the AOD at the required wavelength³⁸.

AOD from MODIS. The MODIS is an important sensor mounted on the Terra and Aqua satellites, which are morning and afternoon satellites, respectively. MODIS satellite data includes information about ground surface albedo, cloud boundaries, atmospheric water vapor, aerosol, surface temperature, and other characteristics³⁹. Satellite coverage in the Central China region cycles twice daily, which means that it can provide data about Central China twice a day. In this study, the MYD_DB and MYD_DT AOD at 550 nm from the MODIS-Aqua Level 2 aerosol data product were obtained, and only the highest-quality-flag (QF = 3) AOD observations were considered for analysis. It should be explained that the wavelengths of MODIS and CALIPSO AOD inversion are different, 550 nm and 532 nm, respectively. However, this difference is around 2–4%, much smaller than the differences between AOD inversion with different instruments⁴⁰. Thus, differences caused by different wavelengths can be neglected in this study.

AOD from CALIPSO. The CALIPSO satellite provides global observational data on aerosol and cloud layers to study the effect of clouds and aerosols on Earth's climate⁴¹. The cycle time of this satellite across the central China region is 16 days. The CALIPSO satellite can detect vertical aerosol extinction profiles and aerosol subtypes including smoke, dust, polluted dust (dust and smoke), and clean and polluted continental and clean marine subtypes³². We used the CALIPSO 5 km Aerosol Layer Product (Level 2, Version 3), which provides aerosol layer optical depth at a wavelength of 532 nm. Moreover, the cases with cloud layer were removed in our comparisons. CALIPSO retrieves AOD based on the scene classification algorithm and the integrated aerosol extinction vertical profile⁴².

Comparison of Methods

According to the statistical methods of other studies^{9,10}, the root-mean-square error (RMSE; Equation (1)), the mean absolute difference (MAD; Equation (2)), and the correlation coefficient (R) were applied to evaluate the uncertainty in aerosol algorithms. The equation of linear regression was used to calculate the slope and intercept of the sample data.

$$RMSE = \sqrt{\frac{1}{n} \sum_{i=1}^n (AOD_{(satellite)i} - AOD_{(ground)i})^2} \quad (1)$$

$$MAD = \frac{1}{n} \sum_{i=1}^n |AOD_{(satellite)i} - AOD_{(ground)i}| \quad (2)$$

The experimental data were collected from November 2013 to December 2017. Based on previous data-matching principles¹⁰, the satellite AOD products were useful when at least 20% of the pixels fell within the ground observation station. Meanwhile, the satellite data compared with sun photometer measurements were the average of satellite AOD products within a range of 20 km at the ground observation station. The ground-based sun photometer data were obtained within 30 min of CALIPSO overpass times. The CALIPSO satellite crosses the ground-based observation station every 16 days. To ensure time synchronization, the MODIS and sun photometer data were screened based on the CALIPSO date. Note that the sun photometer data obtained from Wuhan and Mount Song stations were regarded as ground-based observation data over central China. After the screening process, there were 188 valid matchups cases: 96 and 92 satellite passes within 20 km over the Wuhan and Mount Song stations, respectively.

References

- Albrecht, B. Aerosols, cloud microphysics, and fractional cloudiness. *Science* **245**, 1227–1230 (1989).
- Li, Z. *et al.* Aerosol and monsoon interactions in Asia. *Rev. Geophys.* **54**, 866–929, <https://doi.org/10.1002/2015RG000500> (2016).
- Guo, J. *et al.* Delaying precipitation and lightning by air pollution over the Pearl River Delta. Part I: Observational analyses. *J. Geophys. Res. Atmos.* **121**, 6472–6488, <https://doi.org/10.1002/2015JD023257> (2016).
- Li, J. *et al.* Long-term variation of cloud droplet number concentrations from space-based lidar. *Remote Sensing of Environment*, 144–161 (2018).
- Guo, J. P. *et al.* Three-dimensional structure of aerosol in China: A perspective from multi-satellite observations. *Atmospheric Research* **178–179**, 580–589, <https://doi.org/10.1016/j.atmosres.2016.05.010> (2016).
- Wang, F. *et al.* Multi-sensor quantification of aerosol-induced variability in warm cloud properties over eastern China. *Atmos. Environ.* **113**, 1–9, <https://doi.org/10.1016/j.atmosenv.2015.04.063> (2015).
- Xu, H. *et al.* Warming effect of dust aerosols modulated by overlapping clouds below. *Atmos. Environ.* **166**, 393–402, <https://doi.org/10.1016/j.atmosenv.2017.07.036> (2017).

8. Ma, X. *et al.* Comparison of AOD between CALIPSO and MODIS: significant differences over major dust and biomass burning regions. *J. Atmospheric Measurement Techniques* **6**(9), 2391–2401 (2013).
9. Liu, H. *et al.* Preliminary evaluation of S-NPP VIIRS aerosol optical thickness. *J. Journal of Geophysical Research: Atmospheres* **119**(7), 3942–3962 (2014).
10. Wang, W. *et al.* Validation of VIIRS AOD through a Comparison with a Sun Photometer and MODIS AODs over Wuhan. *J. Remote Sensing* **9**(5), 403 (2017).
11. Belle, J. H. & Liu, Y. Evaluation of Aqua MODIS Collection 6 AOD Parameters for Air Quality Research over the Continental United States. *J. Remote Sensing* **8**(10), 815 (2016).
12. Zarzycki, C. M. & Bond, T. C. How much can the vertical distribution of black carbon affect its global direct radiative forcing?. *J. Geophysical Research Letters*, **37**(20) (2010)
13. Winker, D. M., Pelon, J. & McCormick, M. P. The CALIPSO mission: Spaceborne lidar for observation of aerosols and clouds[C]. *Proc. Spie.* **4893**(1), 1–11 (2003).
14. Winker, D. M. *et al.* Overview of the CALIPSO mission and CALIOP data processing algorithms. *J. Journal of Atmospheric and Oceanic Technology* **26**(11), 2310–2323 (2009).
15. Winker, D. M. *et al.* The global 3-D distribution of tropospheric aerosols as characterized by CALIOP. *J. Atmospheric Chemistry and Physics* **13**(6), 3345–3361 (2013).
16. Xiao, Q. *et al.* Evaluation of VIIRS, GOCI, and MODIS Collection 6 AOD retrievals against ground sunphotometer observations over East Asia. *J. Atmospheric Chemistry and Physics* **16**(3), 1255–1269 (2016).
17. Redemann, J. *et al.* The comparison of MODIS-Aqua (C5) and CALIOP (V2 & V3) aerosol optical depth. *J. Atmospheric Chemistry and Physics* **12**(6), 3025–3043 (2012).
18. Kittaka, C. *et al.* Intercomparison of column aerosol optical depths from CALIPSO and MODIS-Aqua. *J. Atmospheric Measurement Techniques* **4**(2), 131 (2011).
19. Schuster, G. L. *et al.* Comparison of CALIPSO aerosol optical depth retrievals to AERONET measurements, and a climatology for the lidar ratio of dust. *J. Atmospheric Chemistry and Physics* **12**(16), 7431 (2012).
20. Yu, H. *et al.* Global view of aerosol vertical distributions from CALIPSO lidar measurements and GOCART simulations: Regional and seasonal variations. *J. Journal of Geophysical Research: Atmospheres*, **115**(D4) (2010).
21. Liu, C. *et al.* Evaluation of CALIPSO aerosol optical depth using AERONET and MODIS data over China. *Proceedings of SPIE - The International Society for Optical Engineering* **9221**, 92210F–92210F–13 (2014).
22. Liu, B., Ma, Y., Gong, W., Zhang, M. & Yang, J. Study of continuous air pollution in winter over Wuhan based on ground-based and satellite observations. *Atmospheric Pollution Research* **9**(1), 156–165 (2018).
23. Wang, W. *et al.* Deriving Hourly PM_{2.5} Concentrations from Himawari-8 AODs over Beijing–Tianjin–Hebei in China. *Remote Sensing* **9**, 858 (2017).
24. Xiaoyan, M. A. *et al.* Can MODIS AOD be employed to derive PM_{2.5} in Beijing–Tianjin–Hebei over China? *Atmospheric Research* **181**, 250–256 (2016).
25. Lee, K. H. & Kim, Y. J. Satellite remote sensing of Asian aerosols: a case study of clean, polluted, and Asian dust storm days. *J. Atmospheric Measurement Techniques* **3**(6), 1771 (2010).
26. Li, B. *et al.* Comparing MODIS and AERONET aerosol optical depth over China. *J. International Journal of Remote Sensing* **30**(24), 6519–6529 (2009).
27. Chen, W., Fan, A. & Yan, L. Performance of MODIS C6 Aerosol Product during Frequent Haze–Fog Events: A Case Study of Beijing. *J. Remote Sensing* **9**(5), 496 (2017).
28. Ministry of Environmental Protection, Ambient air quality standards (GB3095–2012). Available online: http://www.zzemc.cn/em_aw/Content/GB3095-2012.pdf 2012.
29. Tao, M., Chen, L., Wang, Z., Tao, J. & Su, L. Satellite observation of abnormal yellow haze clouds over East China during summer agricultural burning season. *Atmospheric environment* **79**, 632–640 (2013).
30. Wang, L. *et al.* Aerosol optical properties over mount song, a rural site in Central China. *J.* (2015).
31. Liu, B., Ma, Y., Gong, W. & Zhang, M. Observations of aerosol color ratio and depolarization ratio over Wuhan. *Atmospheric Pollution Research*, **8**(6), 1113–1122 (2017).
32. Omar, A. H. *et al.* The CALIPSO automated aerosol classification and lidar ratio selection algorithm. *J. Journal of Atmospheric and Oceanic Technology* **26**(10), 1994–2014 (2009).
33. Liu, B. *et al.* Two-wavelength Lidar inversion algorithm for determining planetary boundary layer height. *J. Journal of Quantitative Spectroscopy and Radiative Transfer* **206**, 117–124 (2018).
34. Zhang, M. *et al.* Aerosol radiative effect in UV, VIS, NIR, and SW spectra under haze and high-humidity urban conditions. *J. Atmospheric Environment* **166**, 9–21 (2017).
35. Che, H. *et al.* Instrument calibration and aerosol optical depth validation of the China Aerosol Remote Sensing Network. *J. Journal of Geophysical Research: Atmospheres* **114**(D3) (2009).
36. Tao, R. *et al.* Development of an integrating sphere calibration method for Cimel sunphotometers in China aerosol remote sensing network. *J. Particuology* **13**, 88–99 (2014).
37. Eck, T. F. *et al.* Wavelength dependence of the optical depth of biomass burning, urban, and desert dust aerosols. *J. Journal of Geophysical Research: Atmospheres* **104**(D24), 31333–31349 (1999).
38. Wang, L. *et al.* Long-term observations of aerosol optical properties at Wuhan, an urban site in Central China. *J. Atmospheric Environment* **101**, 94–102 (2015).
39. He, Q. *et al.* Validation of MODIS derived aerosol optical depth over the Yangtze River Delta in China. *J. Remote Sensing of Environment* **114**(8), 1649–1661 (2010).
40. Remer, L. A. *et al.* MODIS 3 km aerosol product: algorithm and global perspective. *J. Atmospheric Measurement Techniques* **6**(7), 1829 (2013).
41. Liu, Z. *et al.* The CALIPSO lidar cloud and aerosol discrimination: Version 2 algorithm and initial assessment of performance. *J. Journal of Atmospheric and Oceanic Technology* **26**(7), 1198–1213 (2009).
42. Vaughan, M. A. *et al.* Fully automated detection of cloud and aerosol layers in the CALIPSO lidar measurements. *J. Journal of Atmospheric and Oceanic Technology* **26**(10), 2034–2050 (2009).

Acknowledgements

The authors thank the MODIS team, CALIPSO team, and site managers who provided the data used in the validation analysis. We also acknowledge the Ministry of Environmental Protection of China for providing the real-time air pollutant concentration data (PM_{2.5}). Finally, this work was financially supported by the National Key Research and Development Program of China (2017YFC0212600), the National Natural Science Foundation of China (grant nos 41401498 and 41627804), and the Natural Science Foundation of Hubei Province (2017CFB404).

Author Contributions

The study was completed with cooperation between all authors. Yingying Ma and Liu Boming designed the research topic, Ming Zhang and Liu Boming conducted the experiment and wrote the paper, Wei Wang, Yifan Shi and Wei Gong checked the experimental results. All authors agreed with the submission of the manuscript.

Additional Information

Competing Interests: The authors declare no competing interests.

Publisher's note: Springer Nature remains neutral with regard to jurisdictional claims in published maps and institutional affiliations.



Open Access This article is licensed under a Creative Commons Attribution 4.0 International License, which permits use, sharing, adaptation, distribution and reproduction in any medium or format, as long as you give appropriate credit to the original author(s) and the source, provide a link to the Creative Commons license, and indicate if changes were made. The images or other third party material in this article are included in the article's Creative Commons license, unless indicated otherwise in a credit line to the material. If material is not included in the article's Creative Commons license and your intended use is not permitted by statutory regulation or exceeds the permitted use, you will need to obtain permission directly from the copyright holder. To view a copy of this license, visit <http://creativecommons.org/licenses/by/4.0/>.

© The Author(s) 2018